

# Compact System for High Resolution X-ray Transmission Radiography, In-line Phase Enhanced Imaging and Micro CT of Biological Samples

Jan Jakubek\*, Jiri Dammer, Carlos Granja, Tomas Holy, Stanislav Pospisil, Josef Uher

**Abstract** – Phase imaging visualizes phase shift of photons which passed the sample. Although phase sensitive X-ray imaging offers many advantages it is not routinely used in biological research due to demands of high intensity and highly coherent X-ray beam which is accessible mainly at synchrotron facilities. Phase sensitive imaging can be also carried out with microfocus X-ray tubes. However, the low beam intensity of such systems prolongs the exposure time to such an extent that common digital imaging detectors (CCD, Flat panels) are insufficient due to low efficiency, dark current and noise. This contribution presents a compact phase contrast enhanced imaging system based on a microfocus X-ray tube and the single photon counting pixel detector Medipix2. The spectral sensitivity of the detector together with the polychromatic nature of the beam allows distinguishing an absorption image from a phase image. Spatial resolution of the system can be on the sub micrometer level and measuring times less than a minute. Applications of the system for biological samples are presented. The simplicity of the system allows for routine laboratory work including dynamic in-vivo studies.

## I. INTRODUCTION

Conventional transmission radiography is based on beam intensity attenuation. A fraction of the beam has to be absorbed by the sample in order to obtain an image of its structure. The sensitivity of this method is limited for weakly absorbing objects such as biological samples consisting of soft tissue. On the other hand, phase sensitive imaging uses phase shift of photons which passed the sample (these photons don't contribute to radiation dose). Variations in the phase result from changes in the refractive index across the sample.

The phase of spatially coherent X-ray waves passing an object is shifted according to effective refractive index. The

effective refractive index is an integral of the refractive index along the propagation of the X-rays. Variations in the effective refractive index cause variations in the phase of the transmitted waves. This phase shift deforms the wavefront of the transmitted radiation in a way that the rays are deflected from their original direction of propagation and a loss of intensity is detected in a forward direction.

There are several approaches for phase shift visualization. An interferometric approach uses interference of the transmitted beam with the primary beam. A diffractometric method (DEI) uses an analyzer crystal to separate transmission and phase images. And a so called in-line method separates these at a large object-to-detector distance.

The process of phase contrast imaging causes edge enhancement in the obtained image [2] (see Fig. 1). The technique can be used with monochromatic and even polychromatic X-ray sources [3].

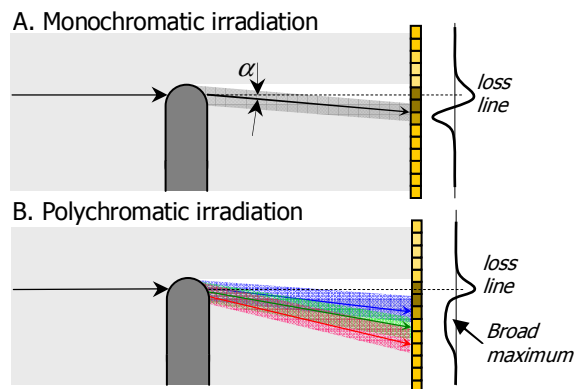


Fig. 1. Principle of in-line phase contrast imaging. Deflection alters the intensity profile of the transmitted beam.

## II. IN-LINE PHASE SENSITIVE IMAGING

Most methods use synchrotron radiation as it can be intensive and monochromatic. However, the in-line technique can be used even with an X-ray tube. If a microfocus X-ray tube is used as an X-ray source, then transversal coherence is assured by the small size of the focal spot.

Manuscript received November 17, 2006. This work has been carried out in frame of the CERN Medipix2 collaboration and was supported in part by the research grant *Collaboration of Czech Republic with CERN* No. 1P04LA211, by the *Fundamental Research Center* project No. LC06041 of the *Ministry of Education, Youth and Sports of the Czech Republic*, by Project 1H-PK2/05 of the *Czech Ministry of Trade and Industry* and by Grant No. 106/04/0567 of the *Grant Agency of the Czech Republic*.

All authors are with the Institute of Experimental and Applied Physics of Czech Technical University in Prague, Horska 3a/22, CZ-12800 Prague 2, Czech Republic (corresponding author: J. Jakubek, telephone: +420-22435-9181, fax: +420-22435-9392, e-mail: jan.jakubek@utef.cvut.cz).

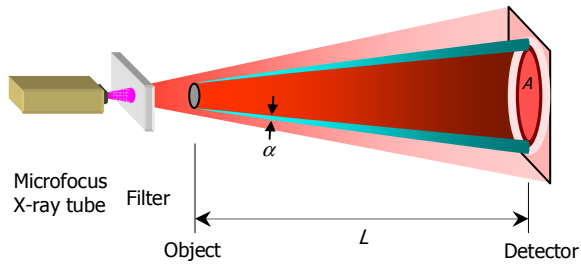


Fig. 2. Setup for in-line phase contrast imaging with microfocus X-ray tube. Distance  $L$  has to be large to distinguish small deflection angle  $\alpha$ .

Since the deflection angle  $\alpha$  is very small (micro radians) the object to detector distance  $L$  (see Fig. 2) has to be large enough to resolve phase contrast effects. The required distance depends on the pixel size, beam energy, object composition and dimension (for  $55\ \mu\text{m}$  pixel size,  $20\ \text{keV}$  X-rays and a small soft tissue object,  $L$  should be at least  $50\ \text{cm}$ ). At such distances, microfocus X-ray tubes cannot provide sufficient beam intensity. Therefore, charge-integrating devices are not suitable for phase contrast imaging. Usage of a highly sensitive and noiseless<sup>1</sup> imaging sensor of the Medipix2 [1] type is advantageous as illustrated in Fig. 3 and 4.

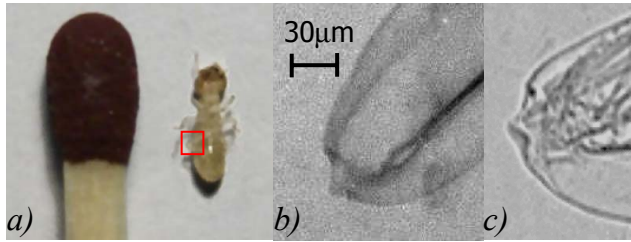


Fig. 3. Photograph of a termite worker (a), X-ray absorption image of termite knee taken by CCD with thin scintillator in contact geometry (b) and same image with edges enhanced by phase effects taken by Medipix2 (c) at a distance of  $60\ \text{cm}$  revealing fine internal structure (Tungsten X-ray tube,  $40\ \text{kV}$ ).

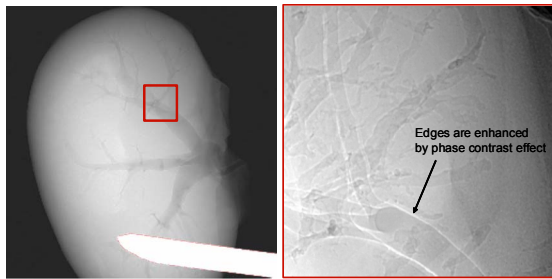


Fig. 4. X-ray transmission image of a mouse kidney (left). Enlarged area with edges enhanced by phase contrast (Medipix2, Tungsten X-ray tube,  $40\ \text{kV}$ ).

The signal caused by phase effects can be for light and therefore almost transparent samples many times larger than the signal caused by absorption (see Fig. 5).

### III. ENERGY DEPENDENCE

The energy dependence of the refractive index differs from the energy dependence of absorption. As Medipix device offers capability of energy discrimination it is possible to

<sup>1</sup> The noise is just of statistical nature.

distinguish whether images are affected by phase shift effects or not<sup>2</sup>. If two images of the same object are measured at two different energy discrimination levels, and both images are translated into equivalent thicknesses<sup>3</sup> [4], then the absorption information contained in both images can be eliminated by subtraction as shown in Fig. 6.

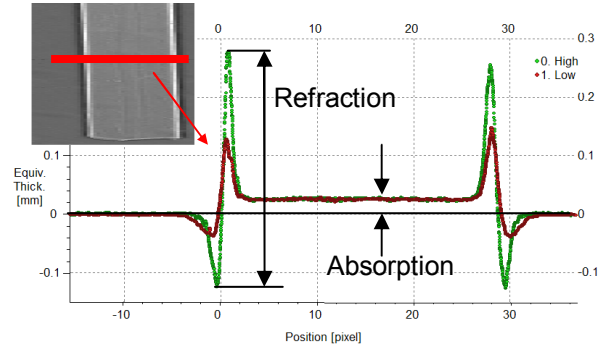


Fig. 5. X-ray image of a  $0.5\ \text{mm}$  thick polyethylene foil strip (inset) and intensity profile along the highlighted line measured with microfocus tungsten X-ray tube at  $40\ \text{kV}$  and Medipix2 detector (object to detector distance was  $70\ \text{cm}$ ). Measurements done at different discrimination levels:  $7\ \text{keV}$  (red) and  $11\ \text{keV}$  (green). Refraction effects are amplified over absorption effects for higher X-ray energy.

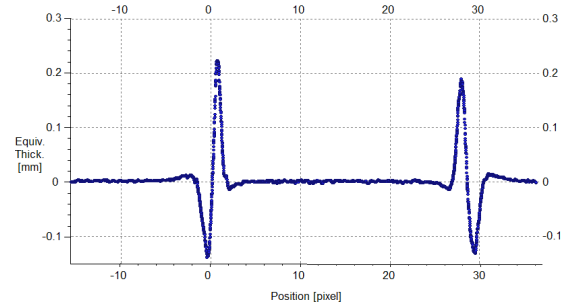


Fig. 6. Subtraction of intensity profiles from Fig. 5. Signal caused by absorption is eliminated.

### IV. SEPARATION OF ABSORPTION AND PHASE

A difficulty of in-line phase contrast radiography with polychromatic irradiation lies in the high complexity of measured images which are a superposition of the absorption image with the phase images for all deflection angles (in contrast to DEI) and all energies. This makes a data interpretation and further evaluation (e.g. tomographic reconstruction) difficult. Using the Medipix2 detector this situation can be simpler. As the detector is energy sensitive (single channel analyzer in each pixel) it is possible to take images for several energies. From these images it is possible to obtain a pure phase image and, a pure absorption image.

#### A. Object idealization

Let us have an ideal object with material composition to allow the use of the method of *Signal to Equivalent Thickness Calibration* (SETC) for image correction [4] (soft

<sup>2</sup> If there are no other energy dependent effects.

<sup>3</sup> Translation is done using signal to thickness calibration method. Calibration has to be done for each discrimination level separately.

tissue object is fine from this point of view). For the SETC method, the response calibration of each detector pixel to the different absorber thicknesses is required. Then, by using a measured calibration function  $c$ , an unknown measured signal (count rate) can be translated to the equivalent absorber thickness.

The second assumption is that the object is thin. Then the changes of the beam propagation direction inside of the object can be neglected thus validating the principle of superposition. Therefore, the sum of two images, each for one object, gives the same result as the image of both objects overlapping each other. In other words: the presence of an additional object will just superpose onto the image.

The validity of the second assumption for real objects was verified by measurement (see Fig. 7). The measurement was done with two polyethylene (PE) objects: a 80  $\mu\text{m}$  thick fiber and a 7.5 mm cylinder. If the assumption would be invalid then the presence of the thick cylinder should deform the image of the fiber or its borders where massive phase effects are observed. The measurement was performed with tungsten X-ray tube at 70 kV. The object to detector distance was about 60 cm. No deformations were observed (Fig. 7 - G and E).

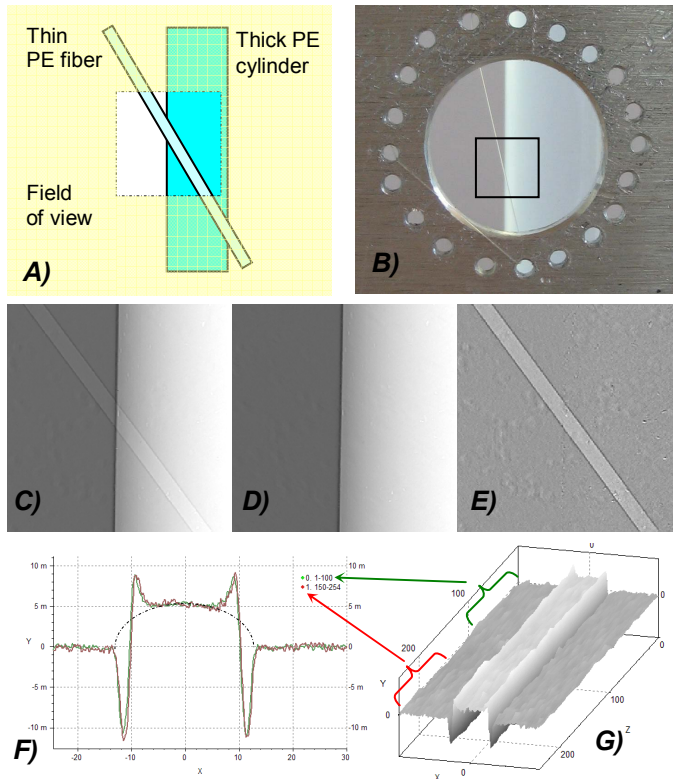


Fig. 7. Two overlapping PE objects simulating soft tissue: Layout schematic (A), photograph (B), X-ray image transformed to equivalent thickness (C), the X-ray image of changed layout – fiber was removed (D), subtraction of both images (E) recovering unaffected image of fiber, the same image in 3D (G) and finally comparison of the two average profiles of the fiber (F) whose differences are of statistical nature.

### B. Mathematical model

**Absorption:** Let us have an object with equivalent thickness given by function  $W(x,y)$  of coordinates  $x$  and  $y$ . In contact

geometry (phase effects are not resolved) we can recover  $W$  from transmission measurement data (count rates)  $T$  by calibration process using the known calibration function  $c$ :

$$W(x, y) = c(T(x, y)) \quad (1)$$

**Refraction:** The effective refractive index of the same object is described by function  $V(x,y)$ . The measurable effects are caused by gradient of effective refractive index  $\nabla V$ . Let us have a completely transparent (zero absorbing) object (ideal phase object). Its transmission image  $P$  is given by some transformation of  $\nabla V$ . Let us denote this transformation as  $p$ . The shape of the transformation  $p$  can be in the general case determined just from measurement of some known objects i.e. by calibration.

$$\nabla V(x, y) = p(P(x, y)) \quad (2)$$

**Combination:** Our object has both properties and the measurement geometry allows resolving phase effects. The measured data  $M$  are composed of two components – an absorption part and a refraction part (which is attenuated by absorption too):

$$M(x, y) = T(x, y) + P(x, y)T(x, y) = T(x, y)(1 + P(x, y)) \quad (3)$$

Using (1) and (2) we can rewrite this term as

$$M(x, y) = c^{-1}(W(x, y))(1 + p^{-1}(\nabla V(x, y))). \quad (4)$$

The equivalent thickness  $W$  can be from (4) expressed as

$$W(x, y) = c\left(\frac{M(x, y)}{1 + p^{-1}(\nabla V(x, y))}\right). \quad (5)$$

**Two different energy spectra:** It is possible to measure the images  $M_1$  and  $M_2$  at different X-ray beam spectra  $S_1$  and  $S_2$  (or at different energy discrimination in the detector). For each spectrum the appropriate calibration functions  $c_1, c_2$  and  $p_1, p_2$  have to be used. The equivalent thickness  $W$  can be expressed from both measurements according to (5). This leads to an equation (skipping  $(x,y)$  for brevity):

$$c_1\left(\frac{M_1}{1 + p_1^{-1}(\nabla V)}\right) = c_2\left(\frac{M_2}{1 + p_2^{-1}(\nabla V)}\right) \quad (6)$$

In regions where  $V$  is constant the phase effect vanishes. In these regions the equality in (6) is obvious. This means that regions where phase effects play a role can be recognized<sup>2</sup> according to a nonzero value of the difference (see Fig. 6):

$$U = c_1(M_1) - c_2(M_2) \quad (7)$$

The goal is to separate the absorption described via equivalent thickness from the phase image i.e. to solve eq. (6).

By skillful selection of the spectra  $S_1$  and  $S_2$  it can be achieved that the significance of phase effect is almost independent i.e.  $p_1 = p_2 = p$ . However, the absorption still differs as much as illustrated by measurement in Fig. 8. This is particularly valid if the differences in the spectra used are caused by different energy discrimination. Then the spectrum  $S_1$  for lower discrimination level contains also the second

spectrum  $S_2$  for higher discrimination. The difference lies in the low energy fraction which is highly attenuated by the object and does not contribute significantly to refraction.

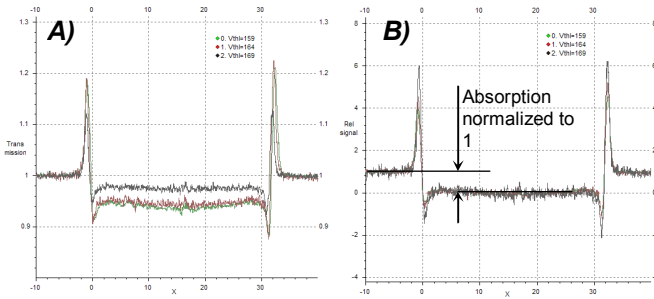


Fig. 8. Measured profiles of the 80  $\mu\text{m}$  thick PE fiber (at higher magnification than shown in Fig. 7) measured at the three energy thresholds: 6 keV, 8 keV and 10 keV (A). Same profiles (B) but normalized and shifted to have absorption signal of 1. This way the phase effect energy dependence is observed. Although transmission signal is highly dependent on threshold settings the phase signal is much less sensitive.

Let us assume that  $p_1=p_2=p$ . Making the substitution

$$q^{(0)} = \frac{1}{1 + p^{-1}(\nabla V)},$$

$$T_1^{(0)} = M_1 \text{ and } T_2^{(0)} = M_2$$

then eq. (6) rewrites as

$$c_1(q^{(0)}T_1^{(0)}) = c_2(q^{(0)}T_2^{(0)}) \quad (8)$$

Both functions  $c_1$  and  $c_2$  are monotonic and smooth. They can be expanded to Taylor series in point  $T^{(0)}$  neglecting members of higher orders:

$$\begin{aligned} c(q^{(0)}T^{(0)}) &= c(T^{(0)}) + c'(T^{(0)})(q^{(0)}T^{(0)} - T^{(0)}) + \dots \approx \\ &\approx c(T^{(0)}) + T^{(0)}(q^{(0)} - 1)c'(T^{(0)}) \end{aligned}$$

With such simplification, eq. (8) can be solved for  $q^{(0)}$ :

$$q^{(0)} = 1 - \frac{c_1(T_1^{(0)}) - c_2(T_2^{(0)})}{T_1^{(0)}c_1'(T_1^{(0)}) - T_2^{(0)}c_2'(T_2^{(0)})} \quad (9)$$

As higher order members in the Taylor series were neglected, the  $p$  computed from  $q^{(0)}$  would be inaccurate. To have a more precise result an iterative process can be used:

$$\begin{aligned} T_1^{(n+1)} &= q^{(n)}T_1^{(n)}, \quad T_2^{(n+1)} = q^{(n)}T_2^{(n)}, \\ q^{(n)} &= 1 - \frac{c_1(T_1^{(n)}) - c_2(T_2^{(n)})}{T_1^{(n)}c_1'(T_1^{(n)}) - T_2^{(n)}c_2'(T_2^{(n)})} \end{aligned} \quad (10)$$

Convergence of this process is very fast. From resulting  $q$  both pure phase image  $P$  and pure absorption image  $T$  (in terms of equivalent thickness) can be easily determined.

The proposed method was experimentally verified by measurements of edge of a PE cylinder with diameter of 7.5 mm. The measurement was performed with the microfocus tungsten X-ray tube at 70kV. The calibration was done with set of aluminum foils of thicknesses 0, 0.05, 0.1 and 0.2 mm. The measurement and the calibration were repeated for two threshold levels: 6keV and 11keV. The results are shown in Fig. 9.

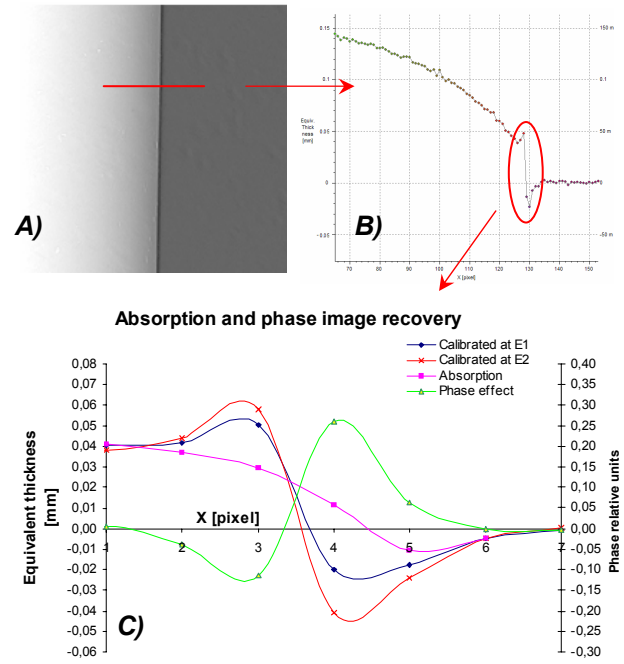


Fig. 9. Experimental verification of absorption and phase image separation from transmission measurements. Transmission image converted to equivalent thickness (A) with marked position of profile (B). Chart (C) shows enlarged profiles taken at two energies (blue and red), computed pure absorption profile (violet) and pure phase profile (green).

## V. CONCLUSIONS

A difficulty of in-line phase contrast radiography with polychromatic irradiation lies in a high complexity of measured images which are superposition of the absorption image and phase images for all deflection angles.

A pure phase image and a pure absorption image can be recovered from X-ray transmission images taken with different energy discrimination by proposed method. For this method the pixel detector with a pair (or more) of independent discriminators and counters such as Medipix3 [5] will be advantageous.

## REFERENCES

- [1] X. Llopart, M. Campbell, R. Dinapoli, D. San Segundo, Pernigotti E.: "Medipix2, a 64k pixel readout with 55  $\mu\text{m}$  square elements working in single photon counting mode", IEEE Trans. Nucl. Sci., 49:2279-2283, 2001. Proc. Conf. Rec. IEEE Nuclear Science Symp. and Medical Imaging Conf. (San Diego, CA, 4-10 November 2001).
- [2] S. W. Wilkins, et al.: "Phase contrast imaging using polychromatic hard X-rays", Nature 384 (1996) 335.
- [3] T. J. Davis, et al.: "Phase contrast imaging of weakly absorbing materials using hard X-rays", Nature 373 (1995) 595.
- [4] J. Jakubek: "Data Processing and Image Reconstruction Methods for Pixel Detectors", contribution to the 8<sup>th</sup> IWORID, to be published in conference proceedings in special issue of Instruments and Methods in Physics Research Section A.
- [5] R. Ballabriga, M. Campbell, E. H. M. Heijne, X. Llopart, L. Tlustos, "The Medipix3 Prototype, a Pixel Readout Chip Working in Single Photon Counting Mode with Improved Spectrometric Performance", Conference record of Nuclear Science Symposium IEEE 2006 San Diego, Oct–Nov. (2006).